Optimum Detection for a Class of Stationary Meteorological Radars

Fernando Darío Almeida García
Sch. of Elec. and Computer Engineering
University of Campinas
Campinas, SP, Brazil
ferdaral@decom.fee.unicamp.br

Marco Antonio Miguel Miranda
Bradar Indústria S.A.
Campinas, SP, Brazil
marco.miranda@bradar.com.br

José Cândido Silveira Santos Filho
Sch. of Elec. and Computer Engineering
University of Campinas
Campinas, SP, Brazil
candido@decom.fee.unicamp.br

***Abstract*—Recently, an innovative low-cost approach for the construction of meteorological radars has been introduced by exploiting the correlation between the received signals from two fixed wide-beam antennas. Yet, it was then found that a very large amount of signal samples would be required to ensure a satisfactory performance of the proposed radar. On the other hand, it was also envisaged that such a problem could be circumvented by the use of more than two antennas. This work is a first step in this direction, extending the original radar proposal from two to an arbitrary number of antennas. In addition to designing an optimum detector for the new radar, we assess its performance by deriving asymptotic, closed-form expressions for the resulting detection and false-alarm probabilities. As a term of comparison, we also design and analyze a suboptimal detection scheme based on the traditional phased-array approach. Numerical examples are given to validate the provided analysis and to illustrate the performance gain achieved from the use of additional antennas.**

***Index Terms*—Correlation, meteorological radars, optimum detection, stationary antennas.**

I. Introduction

Radar applications have provided important advances in different technological areas, such as remote sensing, meteorology, air traffic control, spatial monitoring, and national security [1]–[3]. In particular, for meteorological applications, three main types of radar exist, in terms of structure and operation mode: (i) the large narrow-beam antenna; (ii) the antenna array; and (iii) spaced antennas. In the first radar type, a horn-shaped antenna and parabolic reflectors with circular aperture are used. The azimuth scanning is obtained by rotating the antenna through a motor, and the elevation scanning is obtained by changing the tilt in each rotation [4]. Because of this, the scanning cycle is relatively long (circa 15–20 min). In addition, this approach requires a very robust mechanical equipment and high maintenance costs. In the second radar type, an equivalent narrow beam is obtained by appropriately controlling the relative phases and amplitudes of each radiating element in the antenna array. Therefore, the beam position can be adjusted electronically, rendering a minimum scanning cycle, generally in the order of microseconds [5], [6]. On the other hand, this approach has a high implementation cost due to the use of a massive number of antenna elements. Finally, the third radar type is a special employment of the second one. In particular, only a few radiating elements of the antenna array are activated to determine the position and the radial velocity of the meteorological phenomenon of interest. Interferometric techniques are then used to properly combine the amplitude and phase information of the received signals [6], [7].

In [8], an innovative low-cost, fast-scanning approach with potential use for nowcasting weather predictions was introduced. The approach is based on two stationary (i.e., fixed) wide-beam antennas. The central idea is to achieve narrow-beam resolution by exploiting the signal correlation between the two wide-beam antennas. Whenever there is a meteorological target in the intersection area between the resolution cells of the two antennas, the received antenna signals are expected to be mutually correlated. Otherwise, these signals are expected to be independent. Therefore, the amount of correlation between the antenna signals may serve as a basis for a detection algorithm. The higher the correlation in the presence of a target, the better the expected detection performance. This correlation has been derived in [8] in terms of radar parameters such as frequency bandwidth, baseline distance, and antenna directivity. Related material on the correlation between received radar signals can be found in [9], [10], although for the different contexts of a single rotating, narrow-beam antenna and polarization diversity, respectively (cf. [8] for more discussion on this).

In [11], an optimum detector was provided for the two-antenna radar scheme proposed in [8]. Also, analytical expressions were obtained for the corresponding probabilities of detection (PD) and false alarm (PFA). However, it was then observed that an extremely large amount of signal samples would be required to render the radar performance acceptable, and that such a problem could be alleviated by increasing the number of antennas.

This work is a first step in that direction. In particular, we generalize the radar scheme investigated in [8], [11] from two to an arbitrary number of antennas, by deriving the optimum detection algorithm and associated closed-form expressions of PD and PFA[1]. Sample cases are presented to show the detection improvement achieved with beyond two antennas. For comparison, a suboptimal detection algorithm is also considered, based on the traditional approach of phased arrays.

[1]The results presented herein have been used to assist in the design of meteorological radar systems for Bradar Indústria S.A., a branch of Embraer Defense and Security.

ISBN 978-90-827970-1-5

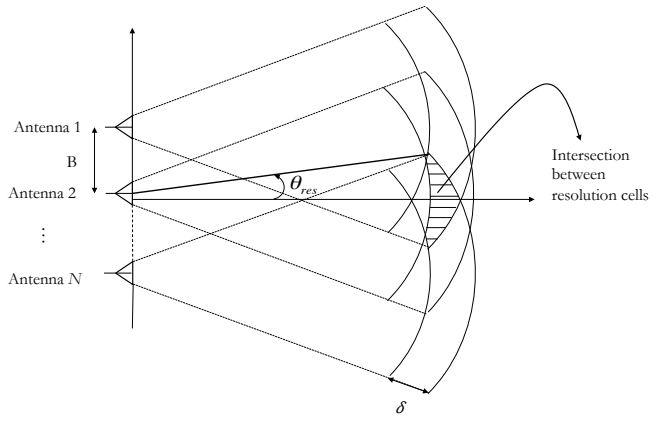

Fig. 1. Top view of the investigated radar system.

This paper is organized as follows. Section II introduces the architecture and the stochastic model of the radar setup; Section III establishes the hypothesis test behind the radar operation; Section IV provides the optimum and suboptimal detection schemes for the proposed radar, as well as corresponding expressions of PD and PFA; Section V discusses some representative numerical results; and Section VI summarizes the main conclusions.

In what follows, $f_{(\cdot)}(\cdot)$ denotes probability density function (PDF); $\mathrm{E}\{\cdot\}$, expectation; $\mathrm{VAR}\{\cdot\}$, variance; $\det(\cdot)$, determinant; $(\cdot)^T$, transposition; and $(\cdot)^{-1}$, matrix inversion.

II. Radar Model

We consider a multi-static radar system composed of N fixed wide-beam antennas. The antennas are aligned and separated by a certain baseline distance B in the azimuth direction, as shown in Fig. 1. A single antenna transmits a linear frequency-modulated pulse, whereas all antennas receive the echo signals. In addition, pulse compression is assumed at the reception [12].

The ability of a radar system to resolve two targets over range, azimuth, or elevation defines its resolution cell [2]. Fig. 1 shows a top view of the range-azimuth resolution cells of each antenna, for a given range distance. The resolution cells form an intersection (hatched) region, inside of which the existence or absence of targets is to be determined. Therefore, the angular span of the intersection region gives the equivalent azimuthal resolution θ_{res} of the radar system. Note that θ_{res} decreases as the number N of antennas increases. This should be considered in practice for a proper radar design. In meteorological applications, $\theta_{\text{res}} < 2^{\text{o}}$ is typically required. As for the range resolution δ, this is given by $\delta = c/(2\Delta f)$ from the assumption of pulse compression, where c is the speed of light and Δf is the bandwidth of the transmitted signal [2].

The signal received by each antenna is a sum of the echoes coming from a large amount of scatterers within the resolution cell. These scatterers represent the meteorological phenomenon under observation (e.g., rain or clouds). Already taking into account the presence of noise and clutter, the signals received by the antennas can be written as

$$S_{k,i} = X_{k,i} + jY_{k,i} \tag{1}$$

where $i \in \{1, \ldots, n\}$ is a discrete-time index, n is the number of samples observed in each antenna, $X_{k,i}$ is the in-phase component at the k-th antenna, and $Y_{k,i}$ is the associated quadrature component, $k \in \{1, \ldots, N\}$. As argued in [8], $X_{k,i}$ and $Y_{l,i}$ are mutually independent random processes, $\forall(k,l)$. In addition, assuming that the pulse repetition interval is much larger than the coherence time associated with the random motion of the scatterers, $S_{k,i}$ is independent of $S_{l,m}$, $\forall(k,l)$ and $\forall i \neq m$ [13]. On the other hand, depending on the absence or existence of a target in the intersection region among the antennas' resolution cells, $X_{k,i}$ and $X_{l,i}$, as well as $Y_{k,i}$ and $Y_{l,i}$, $\forall k \neq l$, can either be mutually independent or bear a certain correlation coefficient ρ_{kl}, respectively. Finally, under quite general conditions, $S_{k,i}$ can be modeled as a circularly symmetrical Gaussian random process, $\forall k$. Herein, for simplicity, we also consider that $S_{k,i}$ and $S_{l,m}$ are identically distributed, $\forall(i,k,l,m)$.

The signal variance and the correlation coefficient ρ_{kl} for an arbitrary pair of antennas have been fully characterized in [8] as a function of the radar's relevant physical parameters. Hence, no further discussion on this topic shall be presented here. Instead, our aim is to design and analyze an optimum detector for the proposed extended radar setup, in terms of arbitrary values of the variance and ρ_{kl}, $k,l \in \{1, \ldots, N\}$. This is attained in the next section.

III. Hypothesis Test

The fundamental problem of a radar system is to decide for the absence or existence of a target. In our case, this problem is posed over each intersection region among the antennas' resolution cells, for multiple range combinations (cf. Fig. 1). In so doing, the radar system scans the entire sector illuminated by the antennas. For simplicity, the observables S_{ki} defined in (1) shall be denoted in compact form as

$$\begin{aligned}\underline{X} \triangleq [&X_{1,1}, X_{2,1}, \ldots, X_{N,1}, X_{1,2}, X_{2,2}, \ldots, X_{N,2}, \ldots,\\ &X_{1,n}, X_{2,n}, \ldots, X_{N,n}]\\ \underline{Y} \triangleq [&Y_{1,1}, Y_{2,1}, \ldots, Y_{N,1}, Y_{1,2}, Y_{2,2}, \ldots, Y_{N,2}, \ldots,\\ &Y_{1,n}, Y_{2,n}, \ldots, Y_{N,n}]\,.\end{aligned} \tag{2}$$

We have the following binary hypothesis test:

- Hypothesis $\mathcal{H}_0$: target is absent. In this case, from the radar model described in the previous section, $\underline{X}$ and $\underline{Y}$ are formed by mutually independent Gaussian components with zero mean and variance σ_0^2.
- Hypothesis $\mathcal{H}_1$: target is present. In this case, $\underline{X}$ is still independent of $\underline{Y}$, but now $X_{k,i}$ and $X_{l,i}$ (as well as $Y_{k,i}$ and $Y_{l,i}$) are jointly Gaussian random variables with zero mean, variance σ_1^2, and correlation coefficient ρ_{kl}. It is worth noting that $\sigma_1^2 > \sigma_0^2$, since σ_1^2 represents the variance of noise plus target echo, whereas σ_0^2 represents the variance of noise alone.

ISBN 978-90-827970-1-5 © EURASIP 2018

IV. Detection Schemes

A. Optimum Detection

The joint PDF of $\underline{X}$ and $\underline{Y}$ can be written as [14]

$$f_{\underline{X}\underline{Y}}\left(\underline{X},\underline{Y}|\mathcal{H}_\nu\right) = \frac{1}{\left((2\pi)^N \det\left(\mathcal{M}_{\mathcal{H}_\nu}\right)\right)^n} \times \exp\left[-\frac{1}{2}\sum_{i=1}^{n}\left(\underline{X}_i{}^T \mathcal{M}_{\mathcal{H}_\nu}{}^{-1}\underline{X}_i + \underline{Y}_i{}^T \mathcal{M}_{\mathcal{H}_\nu}{}^{-1}\underline{Y}_i\right)\right], \tag{3}$$

where $\nu \in \{0,1\}$, depending on the hypothesis, $\underline{X}_i \triangleq [X_{1i}\ X_{2i}\cdots X_{Ni}]^T$, and $\underline{Y}_i \triangleq [Y_{1i}\ Y_{2i}\cdots Y_{Ni}]^T$. In addition, $\mathcal{M}_{\mathcal{H}_0} \triangleq \sigma_0^2\mathbf{I}$ and $\mathcal{M}_{\mathcal{H}_1} \triangleq \sigma_1^2\Sigma$ are the covariance matrices of $\underline{X}_i$ (as well as $\underline{Y}_i$) under each hypothesis, with $\mathbf{I}$ being the identity matrix and

$$\Sigma \triangleq \begin{bmatrix} 1 & \rho_{12} & \rho_{13} & \cdots & \rho_{1N} \\ \rho_{21} & 1 & \rho_{23} & & \rho_{2N} \\ \rho_{31} & \rho_{32} & 1 & & \rho_{3N} \\ \vdots & & & \ddots & \vdots \\ \rho_{N1} & \rho_{N2} & \rho_{N3} & \cdots & 1 \end{bmatrix}. \tag{4}$$

Note that $\mathcal{M}_{\mathcal{H}_0}$ and $\mathcal{M}_{\mathcal{H}_1}$ are $N \times N$ symmetrical matrices.

1) Detection Design: In a binary hypothesis test, the optimum decision (i.e., one that maximizes PD for any given PFA) is established by the Neyman-Pearson Lemma [14]. According to this, the system decides for $\mathcal{H}_1$ whenever the likelihood ratio test (LRT) of $\mathcal{H}_1$ over $\mathcal{H}_0$ exceeds a certain threshold, say γ', and it decides for $\mathcal{H}_0$ otherwise. In other words,

$$\Lambda_{\text{opt}} \triangleq \frac{f_{\underline{X}\underline{Y}}\left(\underline{X},\underline{Y}|\mathcal{H}_1\right)}{f_{\underline{X}\underline{Y}}\left(\underline{X},\underline{Y}|\mathcal{H}_0\right)} \underset{\mathcal{H}_0}{\overset{\mathcal{H}_1}{\gtrless}} \gamma'. \tag{5}$$

Substituting (3) into (5), and making the necessary simplifications, we obtain

$$\Lambda_{\text{opt}} = \left(\frac{\det\left(\mathcal{M}_{\mathcal{H}_0}\right)}{\det\left(\mathcal{M}_{\mathcal{H}_1}\right)}\right)^n \exp\left[-\frac{1}{2}\sum_{i=1}^{n}\left(\underline{X}_i^T\mathcal{M}\underline{X}_i + \underline{Y}_i^T\mathcal{M}\underline{Y}_i\right)\right], \tag{6}$$

where $\mathcal{M} \triangleq \mathcal{M}_{\mathcal{H}_1}^{-1} - \mathcal{M}_{\mathcal{H}_0}^{-1}$.

For simplicity, we use equivalently the so-called log-LRT representation, given as [1]

$$\ln\left[\Lambda_{\text{opt}}\right] \underset{\mathcal{H}_0}{\overset{\mathcal{H}_1}{\gtrless}} \ln\left[\gamma'\right]. \tag{7}$$

Now, absorbing the terms that do not depend on $\underline{X}_i$ and $\underline{Y}_i$ into a new corresponding decision threshold, γ, we can reformulate the decision rule as

$$W \underset{\mathcal{H}_0}{\overset{\mathcal{H}_1}{\gtrless}} \gamma, \tag{8}$$

where W is the new decision variable, obtained as

$$W \triangleq -\frac{1}{n}\sum_{i=1}^{n}\left(\underline{X}_i^T\mathcal{M}\underline{X}_i + \underline{Y}_i^T\mathcal{M}\underline{Y}_i\right). \tag{9}$$

2) Detection Analysis: From the Central Limit Theorem, W approaches a Gaussian distribution as the amount of signal samples approaches infinity [14]. In what follows, we consider that n is large enough to render the Gaussian assumption a good approximation, thereby allowing for an asymptotic performance analysis of the proposed radar system[2]. In this case, W can be fully characterized by its mean value and variance under each hypothesis, as calculated next.

For convenience, we obtain each element of Σ^{-1} in terms of the correlation matrix Σ as [15]

$$\Sigma^{-1}_{(p,q)} = \frac{(-1)^{p+q}\det\left(\tilde{\Sigma}\left[p,q\right]\right)}{\det\left(\Sigma\right)}, \tag{10}$$

with $(\cdot)_{(p,q)}$ denoting the element at the p-th row and the q-th column of a matrix, and $\tilde{\Sigma}\left[p,q\right] \in \mathbb{R}^{(N-1)\times(N-1)}$ being an auxiliary matrix obtained by removing the p-th row and the q-th column of Σ.

Now, using (4), (9), and (10), and applying the Laplace Theorem [15], we eventually show that the mean values of W under each hypothesis are given by

$$\mathrm{E}\{W|\mathcal{H}_0\} = 2\left(N - \frac{\sigma_0^2}{\sigma_1^2\det\left(\Sigma\right)}\sum_{p=1}^{N}\det\left(\tilde{\Sigma}\left[p,p\right]\right)\right) \tag{11}$$

$$\mathrm{E}\{W|\mathcal{H}_1\} = 2N\left(\frac{\sigma_1^2}{\sigma_0^2} - 1\right), \tag{12}$$

and that the corresponding variances are given by (13) and (14), displayed at the top of the next page, where $\mathrm{sgn}\left(\cdot\right)$ represents the sign function.

From (11)–(14), PFA and PD can be finally obtained with use of the following general formulas for a Gaussian decision variable along with a binary threshold detector [2]:

$$\text{PFA} = Q\left(\frac{\gamma - \mathrm{E}\{W|\mathcal{H}_0\}}{\sqrt{\mathrm{VAR}\{W|\mathcal{H}_0\}}}\right) \tag{15}$$

$$\text{PD} = Q\left(\frac{\gamma - \mathrm{E}\{W|\mathcal{H}_1\}}{\sqrt{\mathrm{VAR}\{W|\mathcal{H}_1\}}}\right), \tag{16}$$

where $Q(x) \triangleq \int_x^\infty (1/\sqrt{2\pi})\exp(-t^2/2)dt$ is the complementary cumulative distribution function of a standard (zero mean, unit variance) Gaussian random variable.

B. Phased-Array Detection

In this section, for comparison, we consider a suboptimal detection scheme based on the operation mode of a traditional phased array. In such a radar, each antenna element is assigned a certain gain and a certain phase shift, with the resulting antenna signals being added at the processing stage [6]. For simplicity, and to render a fair comparison with the optimum detector, here we assume a unity gain and a null phase shift for all antenna elements. Like for the optimum detector, we consider a collection of n signal samples for each of the N antennas. Therefore, the received signals can be written as

$$\underline{S} = \sum_{k=1}^{N}\left(\underline{X_S}_k + j\underline{Y_S}_k\right), \tag{17}$$

[2]As shall be seen from the numerical examples, the Gaussian assumption proves to be very accurate for practicable values of n, say, 100–200 samples.

ISBN 978-90-827970-1-5 © EURASIP 2018

$$\mathrm{VAR}\{W|\mathcal{H}_0\} = \frac{4\sigma_0^4}{n}\left(\sum_{p=1}^{N}\left(-\frac{1}{\sigma_0^2}+\frac{\det\left(\tilde{\Sigma}\left[p,p\right]\right)}{\sigma_1^2\det\left(\Sigma\right)}\right)^2+\frac{1}{\sigma_1^4\det\left(\Sigma\right)^2}\sum_{\substack{p=1\\p<q}}^{N-1}\sum_{q=2}^{N}\det\left(\tilde{\Sigma}\left[p,q\right]\right)^2\right) \tag{13}$$

$$\mathrm{VAR}\{W|\mathcal{H}_1\} = \frac{2\sigma_1^4}{n}\left(\sum_{\substack{p=1\\p\le q}}^{N}\sum_{q=1}^{N}\sum_{\substack{r=1\\r\le s}}^{N}\sum_{s=1}^{N}\left(|\mathrm{sgn}(p-q)|+1\right)\left(\frac{(-1)^{p+q}\det(\tilde{\Sigma}\left[p,q\right])}{\sigma_1^2\det(\Sigma)}-\frac{\mathbf{I}_{(p,q)}}{\sigma_0^2}\right)\right.$$
$$\left.\times\left(|\mathrm{sgn}(r-s)|+1\right)\left(\frac{(-1)^{r+s}\det(\tilde{\Sigma}\left[r,s\right])}{\sigma_1^2\det(\Sigma)}-\frac{\mathbf{I}_{(r,s)}}{\sigma_0^2}\right)\left(\Sigma_{(p,r)}\Sigma_{(q,s)}+\Sigma_{(p,s)}\Sigma_{(q,r)}\right)\right). \tag{14}$$

where $\underline{X}_{S_k} \triangleq [X_{k,1}, X_{k,2}, \cdots, X_{k,n}]^T$ and $\underline{Y}_{S_k} \triangleq [Y_{k,1}, Y_{k,2}, \cdots, Y_{k,n}]^T$. The PDF of $\underline{S}$ can be written as

$$f_{\underline{S}}\left(\underline{S}|\mathcal{H}_\nu\right) = \frac{1}{\left(2\pi N\sigma_{\mathcal{H}_\nu}^2\right)^n}$$
$$\times\exp\left[-\frac{\sum_{i=1}^{n}\left(\left(\sum_{k=1}^{N}X_{k,i}\right)^2+\left(\sum_{k=1}^{N}Y_{k,i}\right)^2\right)}{2N\sigma_{\mathcal{H}_\nu}^2}\right], \tag{18}$$

in which $\sigma_{\mathcal{H}_0}^2 = N\sigma_0^2$ and $\sigma_{\mathcal{H}_1}^2 = \sigma_1^2\mathbf{1}^T\Sigma\mathbf{1}$ represent the variance of the sum of N Gaussian components under the hypotheses $\mathcal{H}_0$ and $\mathcal{H}_1$, respectively, $\mathbf{1} = [1, 1, \cdots, 1]^T \in \mathbb{N}^N$ being the unitary vector.

1) Detection Design: The LRT for the phased array detector is defined as

$$\Lambda_{\text{pha}} \triangleq \frac{f_{\underline{S}}\left(\underline{S}|\mathcal{H}_1\right)}{f_{\underline{S}}\left(\underline{S}|\mathcal{H}_0\right)} \underset{\mathcal{H}_0}{\overset{\mathcal{H}_1}{\gtrless}} \gamma'. \tag{19}$$

Substituting (18) in (19), and after some minor simplifications, we obtain

$$\Lambda_{\text{pha}} = \left(\frac{\sigma_{\mathcal{H}_0}^2}{\sigma_{\mathcal{H}_1}^2}\right)^n\exp\left[\left(\frac{\sigma_{\mathcal{H}_1}^2-\sigma_{\mathcal{H}_0}^2}{2\sigma_{\mathcal{H}_1}^2\sigma_{\mathcal{H}_0}^2}\right)\right.$$
$$\left.\times\sum_{i=1}^{n}\left(\left(\sum_{k=1}^{N}X_{k,i}\right)^2+\left(\sum_{k=1}^{N}Y_{k,i}\right)^2\right)\right]. \tag{20}$$

After applying the log-LRT transformation, and since the term $\frac{\sigma_{\mathcal{H}_1}^2-\sigma_{\mathcal{H}_0}^2}{2\sigma_{\mathcal{H}_1}^2\sigma_{\mathcal{H}_0}^2}$ is always positive, we arrive at a new decision rule in terms of $X_{k,i}$ and $Y_{k,i}$ alone, namely

$$Z \underset{\mathcal{H}_0}{\overset{\mathcal{H}_1}{\gtrless}} \gamma, \tag{21}$$

where

$$Z \triangleq \sum_{i=1}^{n}\left(\left(\sum_{k=1}^{N}X_{k,i}\right)^2+\left(\sum_{k=1}^{N}Y_{k,i}\right)^2\right). \tag{22}$$

2) Detection Analysis: Note that $Z/\sigma_{\mathcal{H}_\nu}^2$ follows a chi-squared distribution with $2n$ degrees of freedom. Therefore, after a simple transformation of variables, we obtain the PDF of Z under each hypothesis as

$$f_Z\left(z|\mathcal{H}_\nu\right) = \frac{\exp\left[-\frac{z}{2\sigma_{\mathcal{H}_\nu}^2}\right]\left(\frac{z}{2\sigma_{\mathcal{H}_\nu}^2}\right)^n}{z\Gamma(n)}, \tag{23}$$

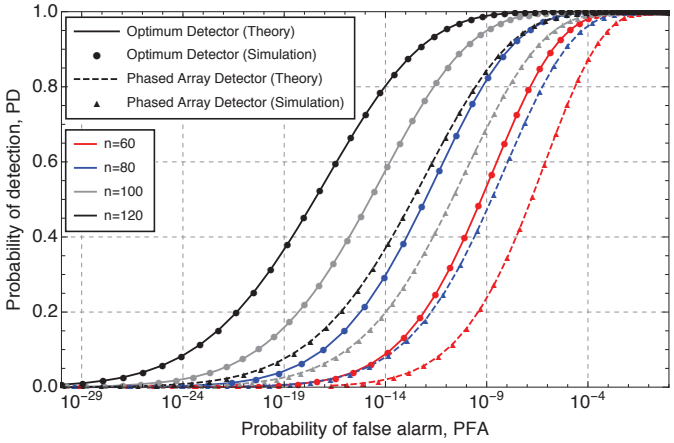

Fig. 2. ROC curves for the optimum and phased-array detectors ($\rho_{12} = 0.5$, $N = 2$, $\sigma_0^2 = 1$, and $\sigma_1^2 = 1.1$).

where $\Gamma(\cdot)$ represents the gamma function. Finally, PFA and PD can be calculated as

$$\text{PFA} = \int_\gamma^\infty f_Z\left(z|\mathcal{H}_0\right)dz = \frac{\Gamma\left(n, \frac{\gamma}{2N\sigma_0^2}\right)}{\Gamma(n)} \tag{24}$$

$$\text{PD} = \int_\gamma^\infty f_Z\left(z|\mathcal{H}_1\right)dz = \frac{\Gamma\left(n, \frac{\gamma}{2\sigma_1^2\mathbf{1}^T\Sigma\mathbf{1}}\right)}{\Gamma(n)}, \tag{25}$$

in which $\Gamma(\cdot,\cdot)$ represents the incomplete gamma function.

V. Numerical Results

In this section we present comparative numerical results in terms of the amount of antennas (N), the amount of signal samples per antenna (n), and the correlation matrix (Σ). The optimum and phased-array detectors we proposed are assessed both analytically and via simulation. For illustration purposes, we consider $\rho_{12} = 0.05$, $\rho_{13} = 0.03$, $\rho_{14} = 0.01$, $\rho_{23} = 0.05$, $\rho_{24} = 0.03$, and $\rho_{34} = 0.05$.

Fig. 2 shows the receiver operating characteristic (ROC) curves for both detectors, with $N = 2$, $\sigma_0^2 = 1$, $\sigma_1^2 = 1.1$, and varying n. Note how the analytical expressions we derived for the detection and false-alarm probabilities of the optimum detector perfectly agree with the simulation results, confirming the validity of the Gaussian assumption for the decision

ISBN 978-90-827970-1-5 © EURASIP 2018

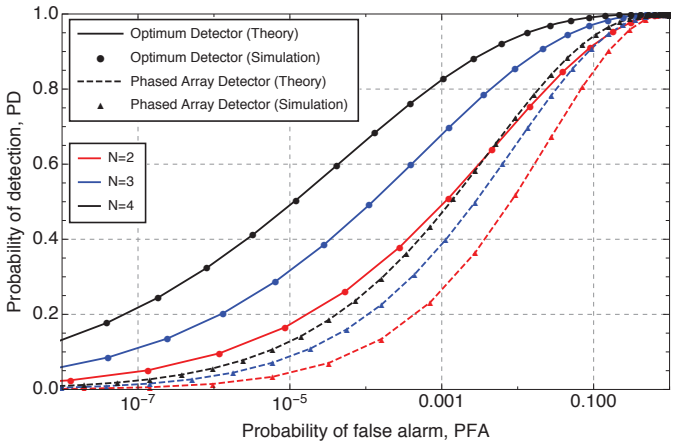

Fig. 3. ROC curves for the optimum and phased-array detectors ($\sigma_0^2 = 1$, $\sigma_1^2 = 1.2$, $n = 100$, $\rho_{12} = 0.05$, $\rho_{13} = 0.03$, $\rho_{14} = 0.01$, $\rho_{23} = 0.05$, $\rho_{24} = 0.03$, and $\rho_{34} = 0.05$).

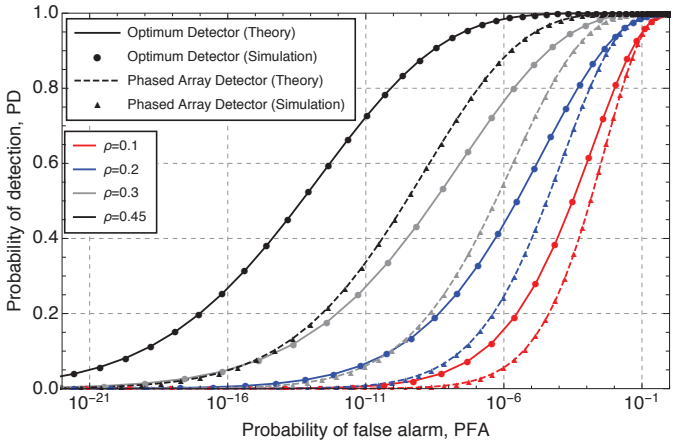

Fig. 4. ROC curves for the optimum and phased-array detectors ($n = 100$, $N = 2$, $\sigma_0^2 = 1$, and $\sigma_1^2 = 1.1$).

variable. Also note the improvement for both detectors as the number of samples increases, and how the optimum detector performs much better than the phased-array detector, yielding a much higher PD for any given PFA. In particular, for PFA $= 10^{-10}$ and $n = 120$, the PD values are 98.1% for the optimum detector and 78.1% for the phased-array detector.

Fig. 3 shows the ROC curves for the optimum detector with two antennas proposed in [11] and the optimum detector with three and four antennas proposed here, for $n = 100$, $\sigma_0^2 = 1$, and $\sigma_1^2 = 1.2$. Once again, note how analytical expressions and simulation results fully match each other, validating (15), (16), (24), and (25). Also note how the optimum detector performs much better with four antennas.

Finally, Fig. 4 shows the ROC curves for the optimum and phased-array detectors with two antennas, $\sigma_0^2 = 1$, $\sigma_1^2 = 1.1$, $n = 100$, and varying $\rho_{12} = \rho$. Note that, as discussed in the Introduction, the performance of each detector improves as the correlation coefficient increases.

VI. Conclusions

In [8] and [11], an innovative approach for the construction of meteorological radars was introduced, based on two fixed wide-beam antennas. In principle, the new approach is cheaper and faster than the traditional one, which is based on a large rotating narrow-beam antenna. However, the former was observed to require an extremely high number of signal samples in order to operate effectively. In this work, we alleviated the referred drawback of this new meteorological radar paradigm by extending it from two to an arbitrary number of antennas. We not only designed the optimum and phased-array detection algorithms for the extended radar setup, but also analyzed their performances in terms of detection and false-alarm probabilities. Our results indicate that the increase in number of antennas brings a considerable performance gain.

References

[1] M. A. Richards, J. Scheer, W. A. Holm, and W. L. Melvin, *Principles of modern radar: Basic principles*, 1st ed. SciTech Pub, 2010.

[2] M. A. Richards, *Fundamentals of radar signal processing*, 2nd ed. McGraw-Hill, 2014.

[3] L. V. Blake, *Radar range-performance analysis*, 1st ed. Artech House, 1986.

[4] M. Wada, J. Horikomi, and F. Mizutani, "Development of solid-state weather radar," in *Proc. IEEE Radar Conference*, California, USA, May 2009, pp. 1–4.

[5] D. S. Zrnic, V. M. Melnikov, R. J. Doviak, and R. Palmer, "Scanning strategy for the multifunction phased-array radar to satisfy aviation and meteorological needs," *IEEE Geosci. Remote Sens. Lett.*, vol. 12, no. 6, pp. 1204–1208, June 2015.

[6] J. Li and P. Stoica, *MIMO radar signal processing*, 1st ed. John Wiley & Sons, 2009.

[7] G. Zhang and R. J. Doviak, "Spaces-antenna interferometry to detect and locate subvolume inhomogeneities of reflectivity: An analogy with monopulse radar," in *Proc. J. Atmos. Ocean. Technol*, Nov. 2008, pp. 1921–1938.

[8] M. A. M. Miranda, J. C. S. Santos Filho, G. Fraidenraich, M. D. Yacoub, J. R. Moreira Neto, and Y. C. Zúñiga, "Correlation between signals from spaced antennas of stationary meteorological radars," *IEEE Trans. Geosci. Remote Sens.*, vol. 52, no. 6, pp. 3116–3124, June 2014.

[9] G. Zhang, R. J. Doviak, J. Vivekanandan, and T. Yu, "Angular and range interferometry to measure wind," *Radio Sci.*, vol. 38, no. 6, pp. 14–1–14–9, Dec. 2003.

[10] A. Ryzhkov, D. Zrnic, J. Hubbert, V. Bringi, J. Vivekanandan, and E. Brandes, "Interpretation of polarimetric radar covariance matrix for meteorological scatterers," in *Proc. Geosci. Remote Sens. Symp.*, vol. 4, 2000, pp. 1584–1586.

[11] M. A. M. Miranda, J. C. S. Santos Filho, G. Fraidenraich, M. D. Yacoub, J. R. Moreira Neto, and Y. C. Zúñiga, "Radar meteorológico com antenas fixas: Projeto e análise de detector ótimo," in *Proc. XXXI Brazilian Symposium of Telecommunications*, Fortaleza, Brazil, 01-04, Sept. 2013.

[12] D. K. Barton, *Radar equations for modern radar*, 1st ed. Artech House, 2013.

[13] H. Sauvageot, *Radar meteorology*. Artech House, 1992.

[14] A. Leon-Garcia, *Probability and random processes for electrical engineering*, 2nd ed. Addison Wesley Longman, 1994.

[15] A. Arnold and I. Guessarian, *Math for computer science*, 2nd ed. Prentice Hall, 1996.

ISBN 978-90-827970-1-5 © EURASIP 2018